BMC Genomics

RESEARCH Open Access

Comparative mitochondrial genome analyses of five medicinal mushroom *Sanghuangporus* provide insights into conservation, variation, and phylogenetic relationships

Can Jin[1], Ying-Yi Ji[1], Lu-Xin Tang[1], Jin-Xin Ma[1], Xin Li[1], Jing Si[1*] and Bao-Kai Cui[1*]

Abstract

Background *Sanghuangporus* species are white-rot basidiomycetes of notable ecological and economic importance, playing critical roles in wood decomposition and medicinal applications. However, comprehensive genus-level mitochondrial genome analyses for *Sanghuangporus* remain limited, which constrains understanding of mitochondrial genome evolution within this lineage.

Results The second- and third-generation sequencing alongside comparative genomic approaches, we analyzed the mitochondrial genomes of five *Sanghuangporus* species (*S. weigelae*, *S. lonicericola*, *S. alpinus*, *S. sanghuang*, and *S. vaninii*). Genome sizes ranged from 97,345 to 116,792 bp, with GC contents between 23.21% and 24.04%. Comparative analyses revealed that mitochondrial genome expansion within the *Hymenochaetaceae* is primarily driven by intron gain. While core protein-coding genes (PCGs) have remained largely conserved, rearrangements were detected in intergenic regions, highlighting the dynamic structural evolution of these fungal mitochondrial genomes. Phylogenetic analyses based on concatenated PCGs and *cox*1 robustly resolved *Sanghuangporus* as a monophyletic clade. Among the conserved PCGs, *atp*9 and *nad*4L exhibited the lowest genetic divergence, all genes displayed *Ka/Ks* ratios < 1, indicating that they were under pervasive purifying selection. Repeat contents, nucleotide diversity, codon usage bias, tRNA secondary structures, and RNA-editing patterns were also characterized.

Conclusion This study provides the first genus-level comprehensive mitochondrial genomic framework for *Sanghuangporus*, illustrating how fungal mitochondrial genomes evolve through intron-mediated expansion, structural rearrangement, and strong functional constraint. Our findings broadly contribute to the understanding of mitochondrial genome evolution in fungi and provide a valuable resource for evolutionary, ecological, and biotechnological studies of medicinally important species.

Keywords *Sanghuangporus*, Mitochondrial genome, Comparative genomics

*Correspondence:
Jing Si
jingsi1788@126.com
Bao-Kai Cui
cuibaokai@bjfu.edu.cn
[1]State Key Laboratory of Efficient Production of Forest Resources, School of Ecology and Nature Conservation, Beijing Forestry University, Beijing 100083, PR China

Introduction

Mushrooms within the genus *Sanghuangporus* are widely distributed across temperate to tropical regions. Also classified as *Phellinus* or *Inonotus*, they have a long history of medicinal use in East Asia [1 – 3]. A taxonomic revision by Zhou et al. [2] established *Sanghuangporus* as a distinct genus within the family *Hymenochaetaceae*, thus resolving longstanding nomenclatural ambiguities arising from excessive synonymy and the frequent misapplication of species names. Accumulating evidence demonstrates that *Sanghuangporus* species produce a diverse array of bioactive metabolites, including polysaccharides, terpenoids, and polyphenols, which confer notable pharmacological properties, including antioxidant, antitumor, antimicrobial, and immunomodulatory effects [4 – 8].

Recent advances in multi-omics approaches have contributed to the elucidation of biosynthetic pathways in *Sanghuangporus*. For instance, integrated transcriptomic, proteomic, and metabolomic analyses revealed the molecular mechanisms underlying unsaturated fatty acid-mediated terpenoid biosynthesis in *S. lonicericola* [9]. Given the scarcity of wild basidiocarp resources, association analyses across multi-stage, genome-wide levels are imperative for the effective exploration of *Sanghuangporus* species and the optimized utilization of its naturally limited wild resources.

Mitochondria are central to cellular energy metabolism and apoptotic regulation and are broadly conserved across eukaryotes [10]. The mitochondrial genome, regarded as the second genome of eukaryotes [11], exhibits significant variation among different organisms [12]. Conserved synthetic blocks, along with the numerous rearrangements occurring within them, can be correlated with major evolutionary events [13]. Recent advances in sequencing technology have accelerated the assembly of mitochondrial genomes, permitting more comprehensive evolutionary and functional investigations.

Fungal mitochondrial genomes remain underrepresented compared to those of plants and animals, particularly within basidiomycetes. Plant mitochondrial genomes display extensive structural diversity, reflecting dynamic evolutionary changes [14 – 17]. Meanwhile, animal mitochondrial genomes and genes have been widely employed in phylogeographic, evolutionary, ancient DNA, and population genetic studies [18 – 20]. Fungi represent a distinct kingdom of organisms and are more closely related to animals than to plants [21]. Despite the large number of Basidiomycota species documented in nature, fewer than 220 mitochondrial genomes from this phylum have been published to date, according to the National Center for Biotechnology Information (NCBI) Organelle Genome Database. Although the mitochondrial genomes of some medicinal mushrooms, such as those of the genera *Ganoderma*, *Inonotus*, and *Phellinus*, have been sequenced [22 – 24], mitochondrial genomic data are available for only two *Sanghuangporus* species – *S. sanghuang* [25] and *S. vaninii* [26]. This scarcity impedes gaining insights into mitochondrial genome evolution and genetic diversity in basidiomycete fungi. While numerous studies have undertaken comprehensive analyses of fungal mitochondrial genomes [27, 28], revealing substantial variation in their genomic architecture–including gene order, repeat content, gene number, and intron composition–even among closely related fungal species [29]. Prior *Sanghuangporus* reports had focused on brief descriptions rather than in-depth characterization [25, 26]. The potential links between *Sanghuangporus* mitochondrial genomic features and critical biological processes, such as growth and development, remain poorly understood, thereby limiting comprehensive exploration of mitochondrial genome biology in medicinal mushrooms.

The present study reports the first comprehensive analysis of the assembly, annotation, and comparison of *Sanghuangporus* mitochondrial genomes. The objectives of this research were as follows: (1) to characterize *Sanghuangporus* mitochondrial genomes, including the similarities, differences, *cox*1 intron dynamic variations, and gene rearrangements among the *Hymenochaetaceae*, using comparative mitochondrial genomics; (2) examine repeat sequences, selective pressure, and nucleotide diversity within *Sanghuangporus* genus; and (3) elucidate the phylogenetic position of *Sanghuangporus* within basidiomycete fungi based on mitochondrial gene datasets. As the first comprehensive comparative mitochondrial genomic study of *Sanghuangporus*, this work advances the understanding of the evolutionary history and genetic diversity of this genus and related taxa within the *Hymenochaetaceae*.

Materials and methods

Sample collection, identification, and sequencing

Fruiting bodies of *S. weigelae*, *S. lonicericola*, and *S. alpinus* were collected from Chongqing, Liaoning, Qinghai, China. Raw sequencing data for *S. weigelae* were obtained from our previous study [30] (BioProject accession number PRJNA1030531) *via* the PacBio Sequel and MGISEQ2000 platforms. The mitochondrial genomes of *S. lonicericola* and *S. alpinus* were sequenced at Beijing Biomarker Technologies Co., Ltd (Beijing, China) on the Illumina NovaSeq 6000 platform. Quality control was applied to raw reads to generate clean data according to a previously published method [31]. The nuclear ribosomal RNA region (18 S-ITS1-5.8 S-ITS2-28 S) for each *Sanghuangporus* species was assembled from the paired-end sequencing data using GetOrganelle v.1.7.7.0 [32] (– R 10 – k 21, 45, 65, 85, and 105 – F fungus_nr). Subsequently,

internal transcribed spacer (ITS) sequences were extracted with ITSx (– preserve T –graphical F), aligned with type specimen sequences (Table S1) *via* MAFFT, and subjected to phylogenetic analyses using the maximum likelihood (ML) and Bayesian inference (BI) algorithms. Two ITS sequences from *Porodaedalea alpicola* (ON358109, ON358110) served as the outgroup for phylogenetic tree reconstruction.

Assembly of mitochondrial genomes

Initially, clean paired-end reads were *de novo* assembled using GetOrganelle v.1.7.7.0 [32] with k-mer values of 21, 33, 55, 77, 99, and 127 (– F fungus_mt), yielding mitochondrial contigs that served as seed sequences. PacBio HiFi reads were then aligned to these seed sequences *via* BLAST, and high-quality candidate sequences were extracted for further assembly using Flye v.2.9.2 [33]. To ensure the reliability of the results, the Flye-assembled sequences were used as targets for iterative assembly. After four rounds of iterative correction and manual inspection, a congruent *S. weigelae* mitochondrial genome length was obtained. NextDenovo [34] was additionally used for reference assembly. The mitochondrial genomes of *S. lonicericola* and *S. alpinus* were assembled using only the initial GetOrganelle v.1.7.7.0 step, followed by manual inspection.

Annotation of mitochondrial genomes

Briefly, protein-coding genes (PCGs), rRNA genes, and tRNA genes in the five *Sanghuangporus* mitochondrial genomes were preliminarily annotated using MFannot [35], MITOS2 [36], and GeSeq [37], with reference to closely related species. tRNA gene prediction was further refined using tRNAscan-SE [38]. RNA-editing sites were predicted with Deepred-mt (probability threshold > 0.9) [39], and all annotations were manually assessed for accuracy. The annotated *S. weigelae*, *S. lonicericola*, and *S. alpinus* mitochondrial genomes were deposited into GenBank under accession numbers PV558911 – PV558913.

Mitochondrial genome features and comparative analysis

BLAST + and BRIG [40] were employed for the comparative visualization of the five *Sanghuangporus* species, with the *S. weigelae* genome serving as reference. Collinearity was assessed using the progressive Mauve algorithm in Mauve v.2.4.0 [41], while conserved and rearranged regions were analyzed with mVISTA [42]. The coding sequence (CDS) length and GC content for 14 PCGs were determined using FastATCG. Additionally, strand asymmetries were calculated using the following formulae: AT skew=(A – T)/(A + T) and GC skew=(G – C)/(G + C).

Repeat sequence analysis

Three categories of repeat sequences, namely, simple sequence repeats (SSRs), tandem repeats, and dispersed repeats, were detected with MISA [43], Tandem Repeats Finder v.4.09 (default parameters) [44], and REPuter (E-value cutoff: 1e-5) [45], respectively. The results of the repeat sequence analyses were visualized using Circos [46].

Intron dynamic analysis

Intron positions within the *cox*1 gene across 16 mitochondrial genomes were compared and visualized using R v.4.3.1. Employing the *cox*1 sequence of *Ganoderma calidophilum* [22] as a reference, intron insertion sites were mapped to classify the *cox*1 genes into distinct positional classes (Pcls). These Pcls were named according to their insertion locations in the reference sequence. Pearson correlation analysis was performed to assess the relationship between *cox*1 intron numbers and gene length across 98 species.

Genetic distance, selective pressure, and nucleotide diversity of the PCGs

Pairwise genetic distances for each PCG were determined in MEGA v.11 [47] under the Kimura-2-parameter (K2P) model. The selective pressure on 14 core PCGs across the five *Sanghuangporus* mitochondrial genomes was evaluated using KaKs_Calculator v3.0 [48] to compute non-synonymous (*Ka*) and synonymous (*Ks*) substitution rates. For nucleotide diversity analysis, PCG sequences were aligned *via* MAFFT, trimmed using Gblocks, and concatenated in PhyloSuite [49]. Nucleotide diversity (Pi) was calculated in DnaSP6 [50] using a sliding window approach, with a window size of 200 bp and a step size of 20 bp.

Codon usage analysis

The PCG sequences extracted from the five *Sanghuangporus* mitochondrial genomes using PhyloSuite were analyzed for codon usage bias with CodonW [51]. The following five indices were calculated: codon adaptation index, frequency of optimal codons, codon bias index, effective number of codons (ENC), and GC content at the third synonymous site (GC3s). ENC-plot analysis (ENC vs. GC3s) was employed to assess the extent of synonymous codon usage bias. The relative synonymous codon usage (RSCU) values were used to identify preferred codons (RSCU > 1) and avoided codons (RSCU < 1). The results were visualized in R v.4.3.1.

Phylogenetic analysis

The mitochondrial genomes for 98 species, including 16 *Sanghuangporus*-related species (Table S2), were retrieved from GenBank based on taxonomic

representation within *Hymenochaetaceae*, phylogenetic affinity to *Sanghuangporus*, and high assembly/annotation quality. Two phylogenetic approaches were employed. First, a combined mitochondrial gene analysis was performed by aligning a concatenated dataset of 14 core PCGs *via* MAFFT and PhyloSuite. *Tremellales* served as the outgroups for the 98-species Basidiomycota dataset, while *Ganoderma* served as the outgroups for the analysis of the 16 *Sanghuangporus*-related species. Fourteen conserved mitochondrial PCGs (*atp*6, *atp*8, *atp*9, *cob*, *cox*1 – 3, *nad*1 – 6, and *nad*4L) were extracted and individually aligned using MAFFT (Alignment Mode: Codon, Code Table: 4) and MACSE (Code Table: 4), implemented in PhyloSuite. The resulting alignments were visually inspected, and poorly aligned or ambiguous regions were removed using Gblocks (Data Type: Codons) under relaxed parameters. The curated alignments were then concatenated into a combined dataset. ML analyses were conducted using IQ-TREE, with the best-fit substitution models selected by ModelFinder [52] under the Akaike Information Criterion for 5,000 bootstrap replicates and the Shimodaira–Hasegawa-like approximate likelihood-ratio test. BI analyses were performed using MrBayes with partitioning schemes and models selected by PartitionFinder2 [53]. These analyses involved two runs with four chains for 2×10^6 generations, a sampling frequency of 100 and a burn-in fraction of 25%. The iterations were assumed to have reached steady state when estimated Bayesian posterior probabilities (BPP) approached 1 and bootstrap supports (BS) reached 100. Genes were treated as separate partitions in the concatenated dataset. Two independent BI runs were conducted with four chains each until convergence was achieved. Subsequently, single-gene analysis was performed by reconstructing separate trees for *cox*1. For both approaches, ML and BI trees were generated. Final trees were visualized in iTOL.

Results

Species identification and assembly quality

The ITS sequences of three *Sanghuangporus* specimens clustered with 2 – 3 specimens of the same species (Fig. S1). The ML and BI algorithms generated nearly congruent topologies (Fig. S1). Based on the analyses of ITS sequences and *Sanghuangporus* morphological features [2]–including perennial, effused-reflexed to pileate basidiocarps; a pileal surface that is brown or dark greyish to black and varies from hispid, tomentose, or velutinate to glabrous with a radially cracked crust; a yellow to brown pore surface; a context that is homogeneous to duplex with a black line; causes a white rot on angiosperm wood) – the newly sequenced specimens were confirmed to be *S. weigela*, *S. lonicericola*, and *S. alpinus*.

The sequencing depth was high and relatively uniform across the three mitochondrial genomes (average depth: *S. weigelae*, ~7027×; *S. lonicericola*, ~1645×; *S. alpinus*, ~2521×). No abrupt coverage drops were observed, and the mismatch and indel rates were low, further confirming that consistency was high between the assembled sequences and the raw sequencing reads (Fig. S2 and Table S3). All quantitative assembly validation metrics indicated that the assembly was reliable.

Features and comparative analysis of five *Sanghuangporus* mitochondrial genomes

The lengths and GC contents of the mitochondrial genomes of the five *Sanghuangporus* species were as follows: *S. weigelae* (116,972 bp, 23.58%), *S. lonicericola* (115,539 bp, 23.31%), *S. sanghuang* (112,060 bp, 23.21%), *S. alpinus* (102,472 bp, 24.04%), and *S. vaninii* (97,345 bp, 23.47%). *S. weigelae* possessed the largest mitochondrial genome, encoding 14 core PCGs, 26 tRNAs, two rRNAs, and one ribosomal protein (*rps*3). These gene counts were consistent with those in other *Sanghuangporus* species, showing only minor variations in tRNA gene numbers (Fig. 1A). Interspecific alignment revealed sequence identity exceeding 70%, indicative of a high level of homology among these species (Fig. 1A). The GC content and GC skew were randomly distributed throughout most of the genomes. As in the synteny analysis, variations and peaks were observed in the similarity comparison (Fig. 1A), which may have implications for mitochondrial function and evolution. An exception occurred at the peaks in unaligned breaks within non-coding regions, where the biased GC skew corresponded to the *S. weigelae* reference mitochondrial genome (Fig. 1A). Mauve identified seven homologous syntenic blocks (I – VII) shared among the five *Sanghuangporus* species (Figs. 1B and S3). Block I, the largest and most conserved region, was present in all five species. This block predominantly harbors a stable number of core PCGs (*cox*1, *nad*4L, *nad*5, *atp*9, *cox*2, *cob*, *cox*3, *atp*6, and *nad*1) and four tRNA genes (*trn*Y, *trn*M, *trn*P, *trn*N, *trn*S, and *trn*I), demonstrating strong structural and functional conservation. Blocks II, Ⅴ, and VII were also detected in all the species but showed moderate variations in length and gene contents. Blocks II and V mainly contain *rrn*L and *nad*4, and adjacent tRNA genes, whereas Block VII encompasses three clusters of tRNA genes (cluster1: *trn*V, *trn*L, *trn*R, and *trn*W; cluster2: *trn*A, *trn*F, *trn*T, and *trn*Q; and cluster3: *trn*M, *trn*D, *trn*G, *trn*R, *trn*M, *trn*E, and *trn*S). In contrast, Blocks III, IV, and VI exhibited variability (Figs. 1B and S8). Specifically, Block III was absent in *S. sanghuang*, *S. alpinus*, and *S. vaninii*. Block IV was missing in *S. alpinus*; and Block VI was lacking in *S. vaninii*. Block V showed orientation differences, including a partial inversion relative to neighboring blocks. Several homologous blocks, particularly

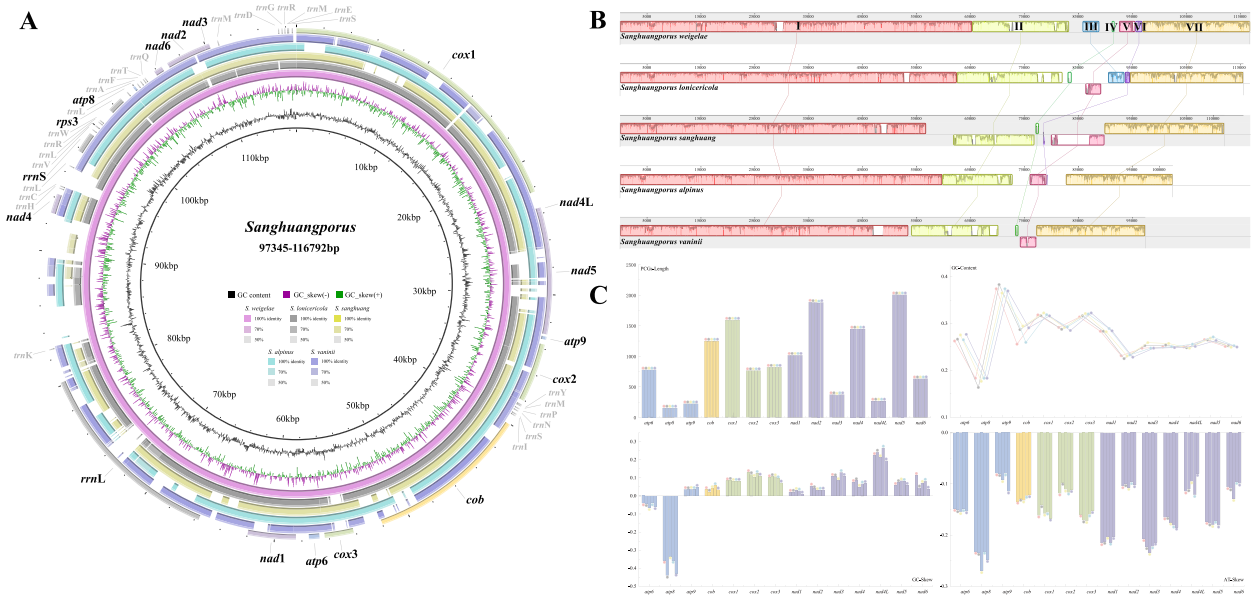

Fig. 1 **A** Alignment of the mitochondrial genomes among the five studied *Sanghuangporus* species. Gaps in the circle represent mismatched sequences in the mitochondrial genome alignment. GC content (black) and GC skew (purple/green) are shown in the innermost two circles. Increased GC content and positive GC skew are represented by peaks oriented toward the center of the circle. Species from inside to outside, color-coded as pink, gray, yellow, blue, and purple, indicate *S. weigelae*, *S. lonicericola*, *S. sanghuang*, *S. alpinus*, and *S. vaninii*, respectively. **B** Collinearity of the mitochondrial genomes in allied species. I–VI represents the homologous regions. **C** Variations in the length and base composition of individual protein-coding genes (PCGs) in the mitochondrial genomes of five *Sanghuangporus* species, including coding sequence (CDS) length variation, GC content, AT skew, and GC skew of the different PCGs

Blocks II – VI, displayed inverted orientations relative to one another across species, and were often flanked by tRNA gene-rich regions. mVISTA analysis highlighted the extent of conservation across species, identifying 19 alignments containing 124 conserved regions in *S. vaninii*, 19 alignments comprising 102 regions in *S. alpinus*, 43 alignments harboring 128 regions in *S. sanghuang*, and 17 alignments with 108 regions in *S. lonicericola* (Fig. S4).

All the mitochondrial genomes contained 14 PCGs (*atp*6, 8, 9, *cox*1 – 3, *cob*, *nad*1 – 6, and *nad*4L), *rps*3, two rRNA genes (*rrn*S and *rrn*L), and a variable number of tRNA genes. The features of the PCGs (CDS length, GC content, GC skew, and AT skew) were highly conserved. The lengths of *cox*1, *nad*2, *nad*3, and *nad*6 varied slightly, whereas those of the other genes were invariant. The longest PCGs were *nad*5 (2,007 bp), followed by *nad*2 (1,872 – 1,887 bp) and *cox*1 (1,587 – 1,590 bp), while *atp*8 (153 bp) was the shortest. The average GC content of the PCGs ranged from 17.78% to 37.30%, with the highest GC content observed in *atp*9 and the lowest in *atp*8. The GC skew was predominantly positive, except in *atp*6 (– 0.065 to – 0.039) and *atp*8 (– 0.333 to – 0.440), while the AT skew was uniformly negative (– 0.270 to – 0.079), varying by gene.

Repeat sequences

The SSRs identified in the five *Sanghuangporus* species are summarized in Table S4. A total of 606 SSR sites were detected across the studied mitochondrial genomes. Most were mononucleotide repeats (61.9%), followed by trinucleotide (10.7%) and tetranucleotide (9.6%) SSRs. The most frequent mononucleotide SSR motif was a thymine (T) repeat, which occurred 193 times and accounted for 51.5% of all mononucleotide SSRs. Among the dinucleotide and trinucleotide repeats, the most common motifs were AT/TA and TTA, respectively. Notably, no mononucleotide guanine (G) repeats were identified in any of the five mitochondrial genomes. The number of SSRs per species ranged from 111 to 143. *S. sanghuang* exhibited the highest number of SSRs (143), followed by *S. weigelae* (121), *S. lonicericola* (119), *S. alpinus* (112), and *S. vaninii* (111). In addition to SSRs, dispersed repeats including forward, palindromic, reverse, and complementary repeat sequences were also detected, with lengths ranging from 30 to 1,341 bp, 30 to 127 bp, 30 to 1,221 bp, 30 to 105 bp, and 30 to 55 bp in *S. weigelae*, *S. lonicericola*, *S. sanghuang*, *S. alpinus*, and *S. vaninii*, respectively (Table S5). Forward repeats were the most frequent, followed by palindromic repeats. For instance, in *S. weigelae*, 24 forward, 18 palindromic, 4 reverse, and 6 complementary repeats were identified, representing 2.92% of its mitochondrial genome (Fig. S5 and Table S5). Additionally, tandem repeats were observed in all species, including 39 in *S. weigelae*, 24 in *S. lonicericola*, 45 in *S. sanghuang*, 25 in *S. alpinus*, and 16 in *S. vaninii* (Table S6). The longest tandem repeat (68 bp, three copies) was

found in the *S. weigelae* mitochondrial genome. Across all five species, most tandem repeats were present in one to three copies. These findings indicated that SSRs and repeat elements are abundant in *Sanghuangporus* mitochondrial genomes.

Intron dynamics, selective pressure, and genetic distance of core PCGs

As the most intron-rich mitochondrial gene in fungi, the *cox*1 is widely used as a model system for investigating intron dynamics, gain and loss events, and intron positional classes. In the present study, a strong Pearson correlation was observed between *cox*1 length and intron number across 98 mitochondrial genomes in Basidiomycota ($r = 0.925$, $P = 7.12 \times 10^{-43}$; Fig. 2A). A total of 127 introns were identified in the *Hymenochaetaceae* mitochondrial genomes, with each species containing between 3 and 15 (Fig. 2B). Within the genus *Sanghuangporus*, intron numbers were uniform across species, together accounting for 37.8% of all identified introns in *Hymenochaetaceae*. This high intron content may contribute to the larger mitochondrial genome sizes observed in *Sanghuangporus*. A Pearson correlation was observed between *cox*1 intron number and whole mitochondrial genome size across 98 mitochondrial genomes in Basidiomycota, ($r = 0.573$, $P = 4.51 \times 10^{-43}$). Orthologous introns at positions P209, P237, P273, P383, P731, P1107, and P1305 were detected in most *Hymenochaetaceae* species. In addition, *Sanghuangporus* mitochondrial genomes exhibited conserved intron positions, and several Pcls (P707, P931, P941) were unique or rare (Fig. 2B).

Analysis of genetic distance revealed that *atp*6 exhibited the highest average pairwise distance (0.062) among the 14 core PCGs in *Sanghuangporus* species, followed by *nad*3 (0.058) and *nad*6 (0.047) (Fig. 2C). The lowest genetic distance (0.013) was observed in *atp*9, followed

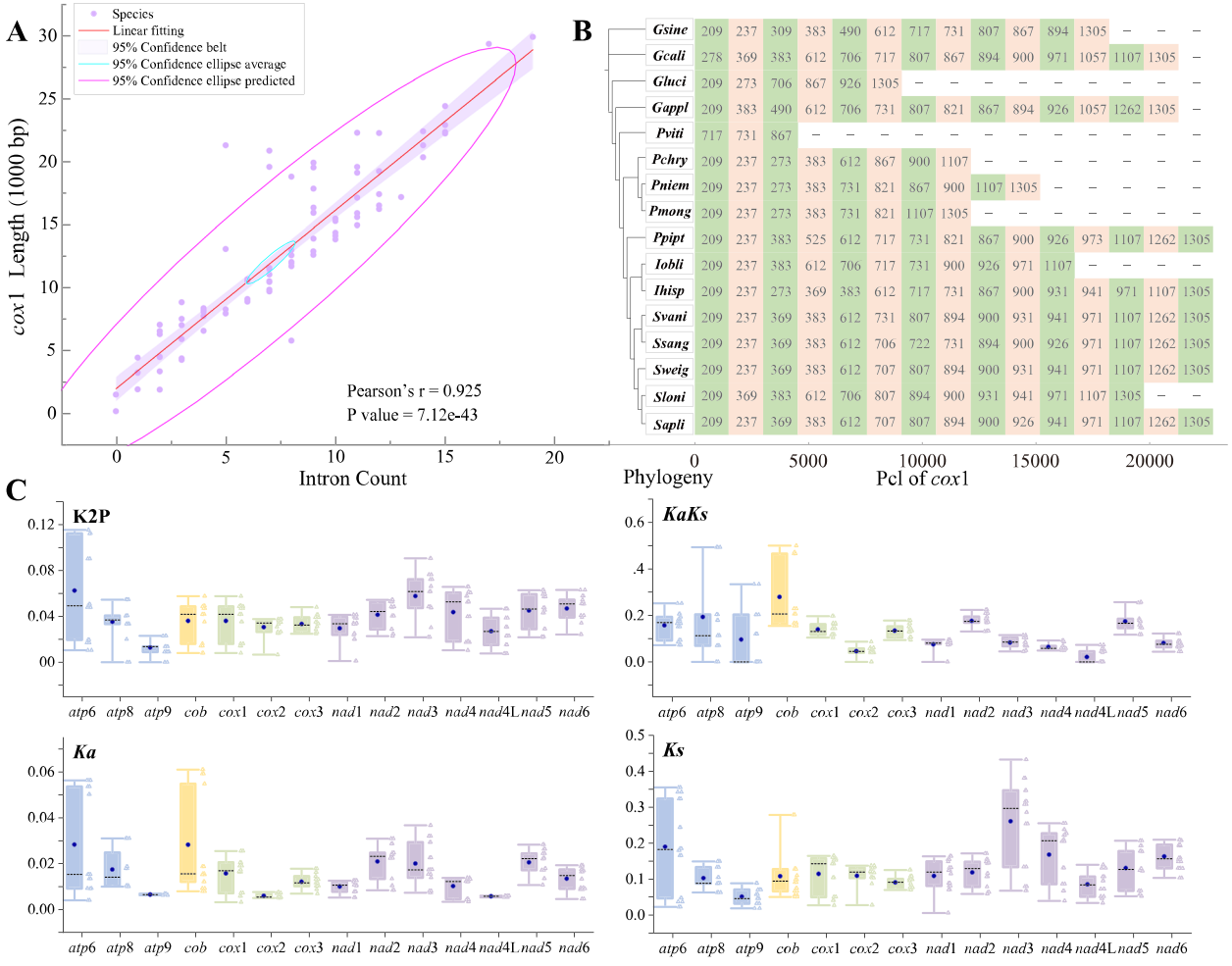

Fig. 2 **A** Pearson correlation analysis between intron number and *cox*1 gene length in the mitochondrial genomes of 98 Basidiomycota species. **B** Positional information for the *cox*1 genes. The left panel shows the phylogenetic positions of *cox*1 gene from 16 species. The right panel shows positional class (Pcl) information for *cox*1. **C** Genetic analysis of the 14 core protein-coding genes (PCGs) conserved in the mitochondrial genomes of five *Sanghuangporus* species. K2P, genetic distance according to the Kimura-2-parameter; *KaKs*, *Ka/Ks* ratio; *Ka*, the mean number of non-synonymous substitutions per non-synonymous site; *Ks*, the mean number of synonymous substitutions per synonymous site

by *nad*4L (0.027), indicating a high level of conservation. Meanwhile, selective pressure analysis of the 14 core PCGs (Fig. 2C) revealed that *cob* had the highest *Ka*/*Ks* ratio (0.279) while *nad*4L displayed the lowest (0.021). Regarding *Ka* values, *cob* exhibited the highest value (0.0283), followed by *atp*6 (0.0282). The highest *Ks* value was observed in *nad*3 (0.260), followed by *atp*6 (0.190), whereas the lowest was recorded in *atp*9 (0.051). Overall, all 14 core PCGs had *Ka*/*Ks* ratios below 1, indicating that they are under purifying selection.

Nucleotide diversity and gene rearrangements

Nucleotide diversity analysis of the 14 core PCGs revealed varying levels of diversity, with Pi values ranging from 0.017 to 0.059 (Fig. 3A). Among these genes, *atp*6 exhibited the highest nucleotide diversity, followed by *nad*3 (Pi = 0.053), *nad*6 (Pi = 0.044), *nad*4 (Pi = 0.042), *nad*2 (Pi = 0.041), *nad*5 (Pi = 0.038), and *cox*1 (Pi = 0.037). In contrast, *atp*9 (Pi = 0.017), *cob* (Pi = 0.023), and *nad*4L (Pi = 0.025) showed relatively low diversity, indicating that these genes possess a higher degree of conservation.

Comparative analyses of mitochondrial gene order across representative genera of *Hymenochaetaceae* revealed both conserved and lineage-specific organizational features (Figs. 3B and S6). All five *Sanghuangporus* mitochondrial genomes exhibited an identical and stable arrangement of the PCGs, rRNA genes, and *rps*3. In contrast, marked differences in gene order were observed

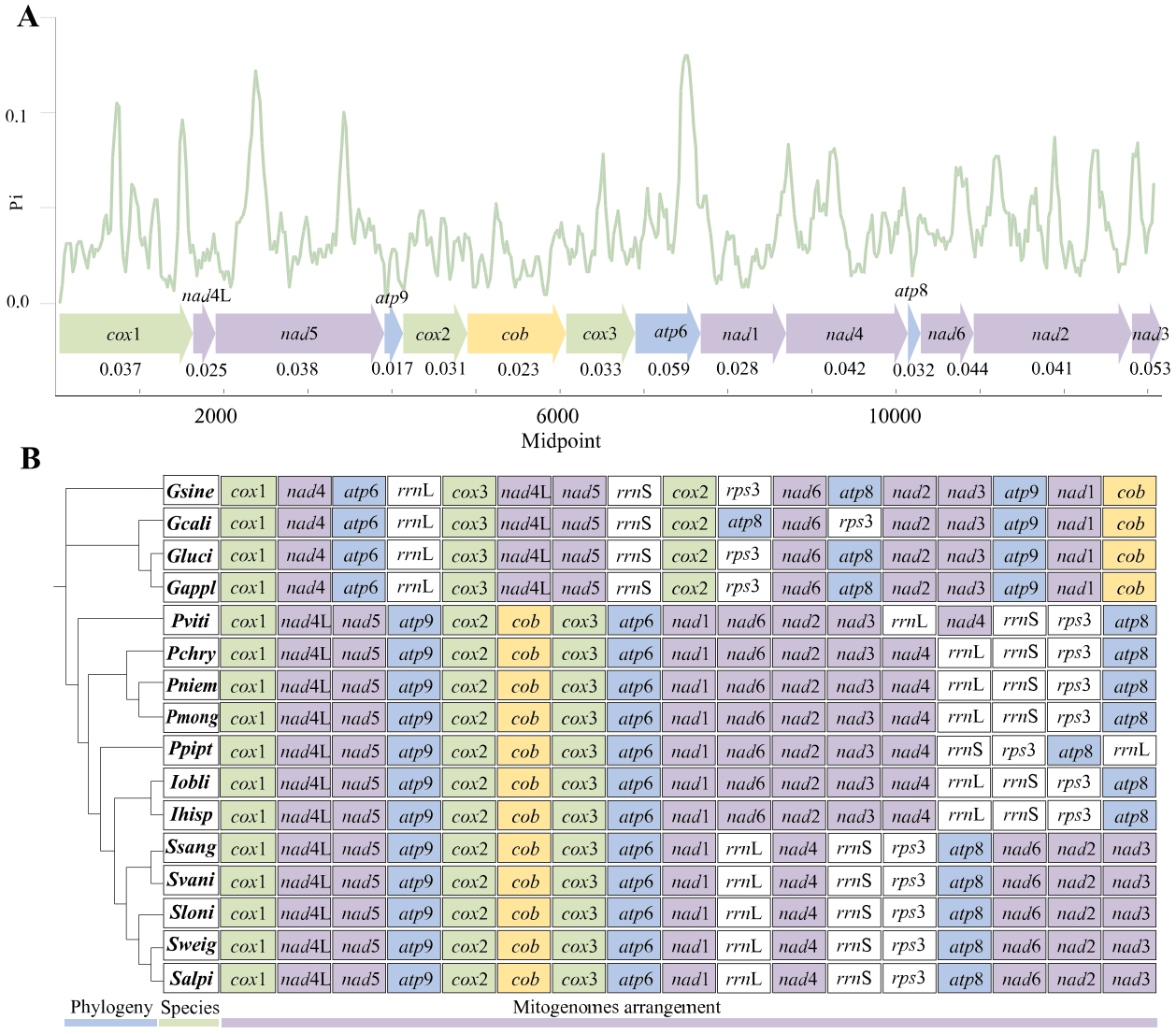

Fig. 3 **A** Nucleotide diversity in the mitochondrial genomes of five *Sanghuangporus* species. The x-axis denotes nucleotide position, while the y-axis denotes nucleotide diversity (Pi). The continuous green line represents Pi values in different protein-coding genes (PCGs) regions. The number above each gene represents its average Pi value. **B** The left panel shows a phylogenetic tree based on concatenated PCGs of the five studied *Sanghuangporus* species. The right panel shows the gene order of each mitochondrial genome, starting with *cox*1. Genes are color-coded as follows: *atp*6, 8, and 9 are shown in blue; *cob* is shown in yellow; *cox*1–3 are shown in green; *nad*1–6 and *nad*4L are shown in purple; and rRNA genes and *rps*3 are shown in white

among different genera within the *Hymenochaetaceae*. *Phellinus* (*Phellinus viticola*), *Porodaedalea* (*Porodaedalea chrysoloma*, *Porodaedalea niemelaei*, and *Porodaedalea mongolica*), *Phellinotus* (*Phellinotus piptadeniae*), and *Inonotus* (*Inonotus obliquus* and *Inonotus hispidus*) each displayed gene clusters and organizations distinct from those of *Sanghuangporus*. A comparative analysis of tRNA genes (Fig. S6) suggested that no lineage-specific rearrangements in these genes occurred within *Sanghuangporus*. However, the few detected tRNA gene variants were predominantly located at rRNA gene regions or at the junctions of *nad*4. These data indicated that mitochondrial genome rearrangements exist at the genus level rather than at the species level. When examining the 14 core PCGs, two distinct gene arrangement patterns were identified upstream of *nad*1 in *Hymenochaetaceae*. These differences involved a positional reversal between two gene clusters, namely, Cluster 1 (*nad*6, *nad*2, and *nad*3) and Cluster 2 (*nad*4 and *atp*8). In *Sanghuangporus*, Cluster 2 was prepositioned adjacent to *nad*1.

Codon usage analysis

The codons UUA (leucine, Leu), AGA (arginine, Arg), CCU (proline, Pro), GCU (alanine, Ala), GGU (glycine, Gly), and UCU (serine, Ser) had the highest RSCU values (Fig. 4A). The frequent use of A- and U-ending codons contributed to the high AT content (average 73.52%) observed in the mitochondrial genomes of the five *Sanghuangporus* species. In *S. weigelae*, 27 codons exhibited a positive usage bias, while 34 displayed a negative usage bias. The RSCU patterns were highly consistent among the analyzed species, with 27, 27, 27, and 26 codons displaying a positive usage bias and 33, 34, 34, and 35 codons exhibiting a negative bias in *S. lonicericola*, *S. sanghuang*,

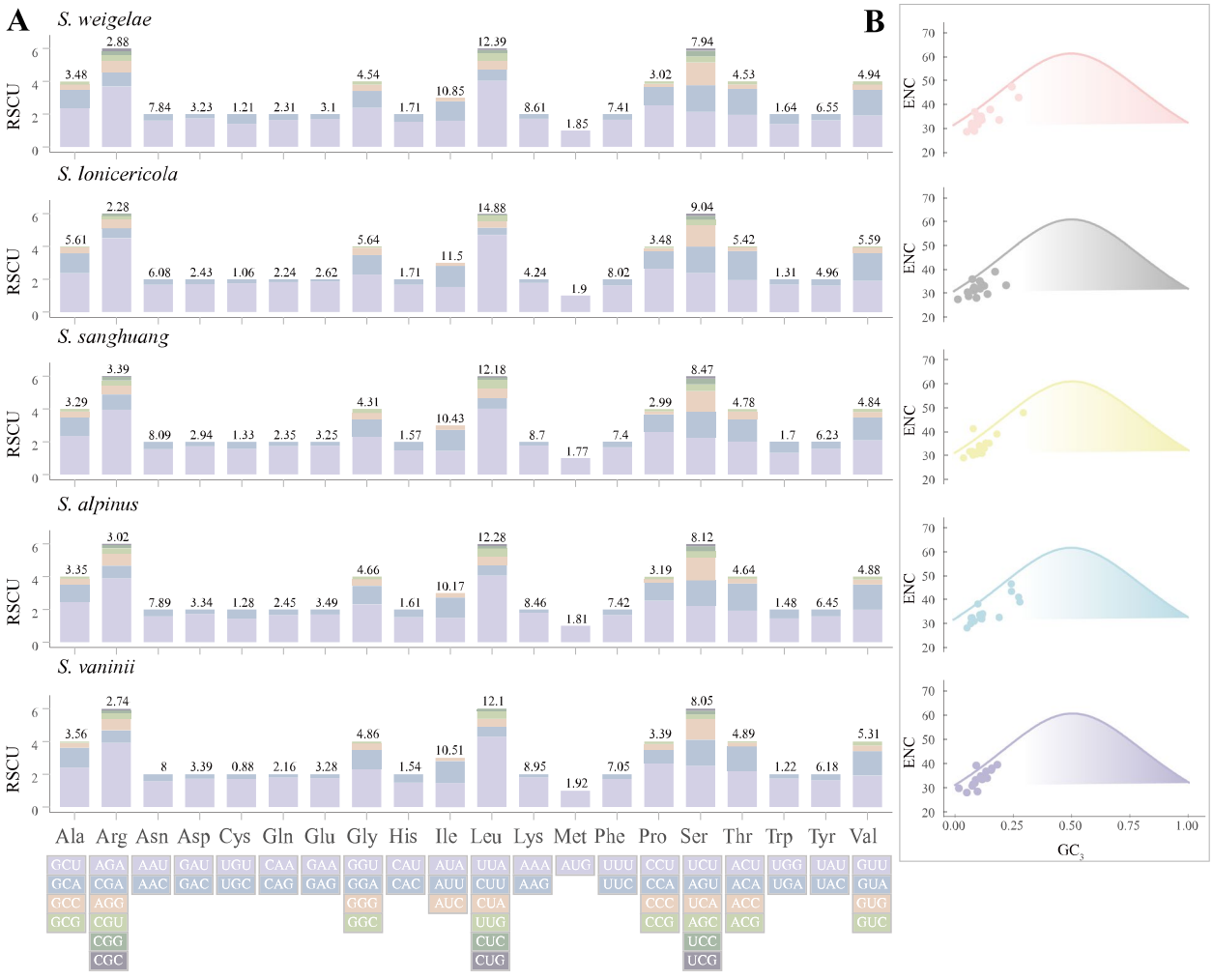

Fig. 4 **A** Relative synonymous codon usage (RSCU) of protein-coding genes (PCGs) in five *Sanghuangporus* species. The frequency of codon usage is plotted on the y-axis, while the x-axis represents codon families. The box at the bottom indicates all codons encoding each amino acid. **B** Plot of the effective number of codons (ENC) illustrating codon usage patterns in the mitochondrial genomes of the five *Sanghuangporus* species. GC3s, GC content at the third codon position

S. alpinus, and S. *vaninii*, respectively (Fig. 4A). Furthermore, codon preference analysis demonstrated that codon bias varied among genes (Fig. 4B). Consistent with the RSCU results, the ENC ranged from 27.81 to 47.71. Moreover, guanine usage was lowest at the third codon position (G3s), with an average frequency of 0.144. The GC3s was 0.44, approximately equal to the overall GC content of 0.46.

tRNA features and RNA-editing sites

A total of 26 tRNA genes were predicted to be present in the mitochondrial genomes of *S. weigelae*, *S. lonicericola*, and *S. alpinus*, while the mitochondrial genomes of *S. sanghuang* and *S. vaninii* contained 27 tRNA genes. The typical set of tRNA genes characteristic of fungal mitochondrial genomes was conserved across *Sanghuangporus* species, including three tRNA genes for methionine (Met), two each for Leu, Ser, and Arg, and one for each of the remaining 16 amino acids. All tRNA genes were dispersed throughout the mitochondrial genomes, and ranged in length from 70 (*trn*M) to 88 (*trn*S) bp. The predicted secondary structures for the 26 tRNAs are shown in (Figs. S7 and S8). Five tRNAs contained extra arm stems. Numerous unmatched base pairs and G – U wobble pairs were present, predominantly localized to the amino acid acceptor arms. Unique tRNA genes were found in *S. lonicericola* (one), *S. sanghuang* (two), and *S. alpinus* (one) (Figs. S7 and S8). Common tRNA genes frequently exhibited structural variations among the five *Sanghuangporus* species (Fig. S8), differing in length and nucleotide sequence.

All RNA-editing sites reported in this study were predicted computationally and have not been experimentally validated with transcriptomic evidence. The 45 predicted C to U RNA-editing sites in the 14 core PCGs in *S. weigelae* and the distribution of the predicted RNA-editing sites in each gene are listed in Table S7. Among these genes, *cox*1, *nad*5, and *nad*2 had the most RNA-editing sites (10, 9, and 7, respectively), while *atp*8, *atp*9, *cox*3, and *nad*4L had none. These findings predicted that 52 amino acids experienced non-synonymous changes, leading to changes in the types of encoded amino acids. The most frequent transition was Ser – Leu, followed by Pro – Leu and Ser–phenylalanine (Phe). A few amino acids–isoleucine, Phe, Leu, Ser, and valine–also underwent synonymous substitutions. The RNA-editing sites involved a total of 20 codon modifications. Among them, 46.67% resulted in amino acid changes with no change in hydrophobicity, 4.44% changed from hydrophobic to hydrophilic, and 37.78% changed from hydrophilic to hydrophobic (Table S8). Comparable RNA-editing profiles were predicted in the other four species of *Sanghuangporus*, with 48, 39, 42, and 46 RNA-editing sites identified in *S. lonicericola*, *S. sanghuang*, *S. alpinus*, and *S. vaninii*, respectively (Table S7). The amino acid changes are presented in Table S8. The proportion of hydrophobic–hydrophobic change was greatest in *S. weigelae*, while hydrophilic–hydrophobic changes predominated in *S. sanghuang*, *S. alpinus*, and *S. vaninii*. *S. lonicericola* had identical proportions of hydrophobic–hydrophobic and hydrophilic–hydrophobic changes.

Phylogenetic analysis

The phylogenetic position of *Sanghuangporus* species and their evolutionary relationships with other basidiomycete fungi were investigated using two datasets: *cox*1 from 16 species and PCGs from 98 species. For each dataset, phylogenetic trees were constructed using BI and ML methods, yielding similar topologies. All major clades in the resulting trees were well-supported, with BPP ≥ 0.99 and BS ≥ 97. Taxonomic analysis based on the five *Sanghuangporus* mitochondrial genomes was undertaken to understand the evolution of *Sanghuangporus* species within the *Hymenochaetaceae*. Generally, high congruence was observed between the ML- and BI-based trees. The *Hymenochaetaceae* formed a monophyletic clade consisting of 12 species, partitioned into three distinct subclades: *Porodaedalea+Phellinus*, *Phellinotus+Inonotus*, and *Sanghuangporus*. *S. lonicericola*, *S. weigelae*, and *S. alpinus* exhibited a close relationship, forming a sister group to the subclade formed by *S. vaninii* and *S. sanghuang* (Fig. 5). Analysis of the mitochondrial phylogenetic tree for the 98 Basidiomycota species showed that the five *Sanghuangporus* species aligned with their established taxonomic classification, consistent with the results obtained for the *cox*1 gene tree (Fig. 2B).

Discussion

This study presents a comprehensive analysis of the mitochondrial genomes of five *Sanghuangporus* species; notably, the mitochondrial genomes of *S. weigelae*, *S. lonicericola*, and *S. alpinus* were newly sequenced in this work. The results revealed that these mitochondrial genomes are defined by notable structural features, conserved elements, and lineage-specific variations, thereby deepening essential insight into the evolutionary history and functional genomics of these economically and scientifically important macrofungi.

The present analysis revealed both conserved and variable features among *Sanghuangporus* mitochondrial genomes, including general mitochondrial genome characteristics, repeat sequences, intron dynamics, selective pressure, genetic distances, nucleotide diversity, gene rearrangements, codon usage biases, tRNA structures, and RNA editing. The high degree of collinearity and sequence similarity observed among the five mitochondrial genomes suggests that these species

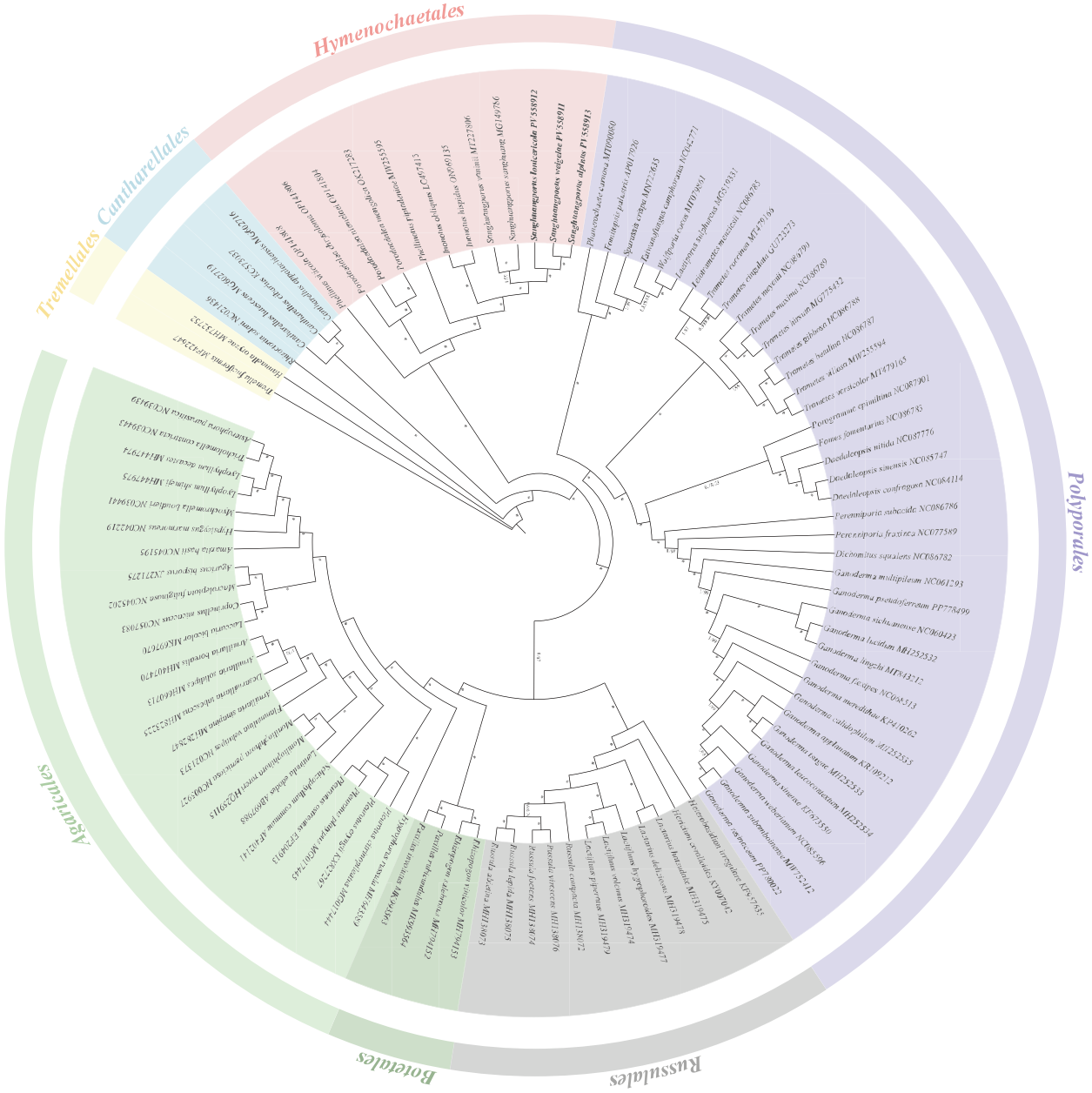

Fig. 5 Molecular phylogeny of the 98 investigated species inferred using Bayesian inference (BI) and maximum likelihood (ML) methods based on the 14 core protein-coding genes (PCGs). Bayesian posterior probabilities (BPP) and ML bootstrap supports (BS) are shown next to each branch. Asterisks (*) indicate nodes with BPP and BL of 1.00 and 100%, respectively. GenBank accession numbers are displayed as suffixes following species names

share an evolutionary origin. Mitochondrial genome sizes ranged from 97,345 to 116,792 bp, indicating slight variation among species (Tables S2). All five species possessed a full set of conserved PCGs essential for mitochondrial function and energy metabolism. Despite small variations, these genes exhibited a high degree of length conservation across species, which is biologically informative. In fungal mitochondrial genomes, PCG length variation is often driven by intron insertions, gene boundary instability, or a consequence of annotation ambiguity. Consequently, the observed pattern consistently indicates that strong functional and structural constraints are acting on core oxidative phosphorylation genes, supporting their suitability for downstream evolutionary and phylogenetic analyses. *S. alpinus* exhibited the highest GC content and had a negative AT/GC skew (except for *atp*8). A gene-level analysis of the GC and AT skews was undertaken to explore strand-specific nucleotide compositional biases associated with mitochondrial replication. The skew patterns were uniform across the conserved PCGs, indicating that replication-associated mutational pressures were stable within

Sanghuangporus. The GC content was consistently low across all species, supporting the hypothesis that shared mutational bias, selection, or recombination-associated DNA repair mechanisms drive these compositional patterns [54]. The narrow GC-content range observed among the five analyzed species indicates that this mutational regime has remained evolutionarily stable since the divergence of extant *Sanghuangporus* lineages. Additionally, uniformly AT-rich mitochondrial genomes are a common feature in basidiomycete fungi and are generally attributed to asymmetric mutation pressure favoring A/T over G/C nucleotides, rather than to lineage-specific adaptive processes [55]. From an evolutionary perspective, persistent AT bias may indirectly shape mitochondrial genome architecture by influencing codon usage patterns, amino acid composition, and the structural properties of non-coding regions [56]. AT-rich sequences are known to facilitate the formation of secondary structures and promote replication slippage or recombination, potentially contributing to the frequent rearrangements observed in intergenic and tRNA-rich regions of fungal mitochondrial genomes [55, 56].

Repetitive sequences are widely recognized as important contributors to structural variation and genomic plasticity in fungal mitochondrial genomes [57]. In the present study, *Sanghuangporus* mitochondrial genomes exhibited a high abundance of SSRs as well as dispersed and tandem repeats. Such repeat-rich regions serve as hotspots for homologous and illegitimate recombination, potentially facilitating genome rearrangements, sequence duplications, and deletion events [58]. Within the *Sanghuangporus* genus, the observed predominance of forward repeats and the presence of long dispersed repeats–exceeding 1 kb in some species–suggest that recombination-driven mechanisms may have contributed to the shaping of mitochondrial genome architecture. However, despite the relatively high repeat content, the overall gene content and gene order among the five *Sanghuangporus* species were highly conserved, reflecting strong functional constraints that limit excessive structural instability. The absence of mononucleotide G repeats and the dominance of A/T-rich SSR motifs may further reflect selective pressures associated with replication fidelity and oxidative damage in mitochondrial genomes, given that G-rich repeats have an elevated propensity for replication slippage and mutational instability [59]. Together, these observations suggest that repeat elements in *Sanghuangporus* mitochondrial genomes contribute to localized sequence variability and structural flexibility, while purifying selection maintains global genome organization. This balance between repeat-mediated plasticity and functional constraint may be essential for mitochondrial genome evolution in *Sanghuangporus* species.

Within the studied order *Hymenochaetales*, *Inonotus hispidus* presented the largest mitochondrial genome (171,046 bp), characterized by a high intron count. The *cox*1 gene is the primary reservoir for introns in the Basidiomycota, and its intron dynamics greatly affect the size of mitochondrial genomes [60]. The present study, encompassing 98 species, revealed a strong positive correlation between *cox*1 intron number and *cox*1 length. Similarly, a positive correlation was observed between the number of introns in whole mitochondrial genomes and the overall mitochondrial genome size in basidiomycetes. These findings suggest that intron accumulation is a primary driver of the expansion of *Sanghuangporus* mitochondrial genomes. Analysis of the 16 analyzed mitochondrial genomes revealed that *cox*1 introns could be classified into different Pcls, with some Pcls sharing across all species, and others occurring rarely and in a species-specific manner. Introns from different species that were assigned to the same Pcl were considered homologous and typically exhibited high sequence similarity [61]. Introns P707 and P807 were unique to *Sanghuangporus*, while others (e.g., P209, P237, and P383) showed homology with distantly related species. These Pcl distributions suggest that a dynamic turnover process, potentially involving intron gain and loss, is occurring within these lineages. However, the precise underlying evolutionary mechanisms cannot be resolved without intro-level phylogenetic analyses. These patterns are consistent with previously reported intron dynamics in fungal mitochondrial genomes, where such fluctuations substantially contribute to genome size variation.

The highest K2P genetic distances were detected in *atp*6 and *nad*3, indicating that these genes have undergone notable evolutionary divergence, while the lowest was observed in *atp*9, reflecting a high level of conservation. This pattern is consistent with the nucleotide diversity results, thereby clarifying the extent of the genetic conservation and evolutionary pressure of each PCG in *Sanghuangporus* mitochondrial genomes. The evolutionary rates, which generally depend on purifying selection, mutation, and directed selection, varied among the core PCGs. The *Ka*/*Ks* ratio was used to estimate the evolutionary selection pressure on the 14 core PCGs within the mitochondrial genomes. As shown in (Fig. 2C), all the PCGs exhibited *Ka*/*Ks* ratios < 1, indicating that they were under pervasive purifying selection, and highlighting the strong evolutionary conservatism of mitochondrial genes across *Sanghuangporus* species. Such strong purifying selection is a normal feature of mitochondrial genomes and reflects functional constraints associated with oxidative phosphorylation [62]. Nucleotide diversity analysis revealed that *atp*9 was highly conserved, as are specific regions within other genes. These findings suggested that these genes play important roles in survival

and evolution. Moreover, different regions showed varying levels of nucleotide diversity, providing valuable information for designing specific-specific primers or conducting evolutionary analyses.

Mitochondrial gene rearrangements have been widely documented and are often associated with recombination, intron mobility, and lineage-specific evolutionary histories [60]. Comparative mitogenomic analyses revealed that gene rearrangements in *Hymenochaetaceae* have predominantly occurred at the intergeneric level, whereas mitochondrial gene order has remained highly conserved within genera. Within *Sanghuangporus*, all examined species shared a nearly identical gene arrangement, even after tRNA genes were included in the analysis. This structural stability suggests that strong evolutionary constraints act on the mitochondrial genomes of this genus, potentially reflecting a relatively recent radiation or limited recombination activity after genus divergence. The conserved gene rearrangement also corresponds well with the monophyly of *Sanghuangporus* as inferred from mitochondrial PCG phylogenies, supporting that gene order conservation is strongly linked with phylogenetic coherence. In contrast, comparisons among different genera revealed multiple rearranged gene blocks, particularly in regions surrounding *nad*6, *nad*4, and *atp*8. Such rearrangements may result from intramolecular recombination facilitated by repetitive elements, introns, or tRNA gene-associated recombination hotspots, as proposed for other fungal lineages. The frequent localization of tRNA genes at block boundaries provided further evidence of their role in mediating recombination events, as shown in the synteny analysis. Overall, these findings suggest that mitochondrial gene rearrangements in *Hymenochaetaceae* are more informative at deeper taxonomic levels and that the highly conserved gene order within *Sanghuangporus* reflects evolutionary stability rather than structural plasticity. Genomic synteny analysis also identified rearrangements within non-coding regions in the five *Sanghuangporus* mitochondrial genomes (Fig. 1B). This variability highlights the dynamic nature of mitochondrial genome architecture, even among congeneric species, as also observed in previous research [22]. While gene order can provide phylogenetic insights, convergent evolution must be considered when interpreting such rearrangements [60]. Further studies are needed to determine their functional consequences, particularly considering the role of mitochondria in energy metabolism.

RSCU analysis showed a consistent preference for A/T at the third codon position across all studied species, a pattern that is also common in higher plants [15 – 17]. Codon bias affects translation efficiency and protein folding, and is thus a key determinant of gene expression and protein structure [63 – 65]. *Sanghuangporus* species exhibit marked consistency in codon usage bias, reflecting strong functional constraints on mitochondrial PCGs and reinforcing the reliability and comparability of gene annotation across taxa. In the ENC-plot analysis, every gene fell below the expected curve, indicating that natural selection, rather than mutational pressure, is the primary force driving codon bias in *Sanghuangporus* mitochondrial genomes, as evidenced by lower ENC values and a pronounced preference for specific codon [66].

Most predicted tRNAs exhibited typical cloverleaf secondary structures, reflecting strong functional constraints on mitochondrial tRNA genes, a pattern widely observed across eukaryotic mitochondrial genes [67, 68]. The predicted RNA-editing sites with minor interspecific variation may potentially influence amino acid properties. These functional proteins after editing ensured the final products achieve closer sequence conservation with homologs in other systems [69, 70]. For instance, in *S. weigelae*, RNA editing altered 37.78% of the amino acids in the mitochondrial genome from hydrophilic to hydrophobic, potentially impacting protein conformation and function [71]. Notably, all RNA-editing sites reported herein were predicted computationally. These sites represent only preliminary hypotheses and provide a reference framework for future transcriptome-based studies designed to validate RNA-editing patterns and explore their functional roles in fungal mitochondrial genomes.

A fundamental objective in biology is the reconstruction of the tree of life [72]. Mitochondrial genomes have been extensively used to infer the tempo and mode of evolutionary changes, as well as the processes underlying speciation and adaptive radiation [12]. Most Basidiomycota species available in the NCBI database were included in the phylogenetic trees in the present study, providing a comprehensive view of the phylogenetics within this phylum. The trees constructed from concatenated PCGs using BI and ML methods were congruent and well-supported. The inferred species relationships were in agreement with current taxonomy, aligning with their historical classification and recent reassignment [2]. In the two trees, *S. lonicericola*, *S. weigelae*, and *S. alpinus* exhibited a close relationship (Fig. 5). This phylogenetic clustering was also consistent with the results for the *cox*1 gene tree (Fig. 2B). While the present results highlight the importance of mitochondrial genome data, more extensive investigations are necessary to determine which phylogenetic method is most accurate for this taxon.

Although the present study provided comprehensive insights into mitochondrial genomes across five *Sanghuangporus* species, there were several limitations. Because mitochondria play a central role in cellular energy production and metabolic regulation [10], evolutionary changes in mitochondrial genomes may have

important functional and ecological implications for ectomycorrhizal fungi. *Sanghuangporus* species form symbiotic associations with woody host plants, a lifestyle that requires efficient energy metabolism to sustain hyphal growth, nutrient exchange, and long-term host colonization. The conservation of core PCGs involved in oxidative phosphorylation across *Sanghuangporus* mitochondrial genomes suggests that strong selective constraints act on energy-generating pathways, reflecting the fundamental metabolic demands of ectomycorrhizal symbiosis. Meanwhile, moderate sequence divergence and variation in non-coding regions, including repetitive elements, may serve as a source of mitochondrial genomic flexibility that facilitates adaptation to different host species or environmental conditions. Such variation could influence mitochondrial transcriptional regulation or replication efficiency, thereby indirectly affecting respiratory performance under fluctuating ecological contexts. Similar patterns have been reported in other ectomycorrhizal and wood-decaying fungi, where mitochondrial genome evolution appears to balance functional conservation with adaptive plasticity. Collectively, these features suggest that mitochondrial genome evolution in *Sanghuangporus* may reflect an adaptive compromise between maintaining essential bioenergetic functions and allowing limited structural and sequence variability to support ecological diversification and host-associated adaptation in ectomycorrhizal fungi. However, a broader sampling of *Sanghuangporus* species and individuals is needed to fully capture interspecific variation. Studies incorporating mitochondrial and nuclear markers could provide a more holistic view of *Sanghuangporus* evolution. Further functional validation of identified repeat elements and rearrangements is also essential. Future work should explore these aspects to enhance the understanding of mitochondrial genomic evolution and support conservation and breeding efforts.

Conclusion

In the present study, the mitochondrial genomes of three *Sanghuangporus* species – *S. weigelae*, *S. lonicericola*, and *S. alpinus*–were sequenced and assembled for the first time. A comprehensive exploration of these mitochondrial genomes, including detailed annotations and comparisons, was undertaken. All *Sanghuangporus* mitochondrial genomes displayed a highly conserved gene complement. Additionally, all the core mitochondrial genes were found to be under purifying selection, highlighting the evolutionary conservatism of mitochondrial energy metabolism. Comparative and synteny analyses uncovered structural stability within mitochondrial gene rearrangements. Phylogenetic investigations based on the *Sanghuangporus* mitochondrial genomes indicated that 98 Basidiomycota species and variants were divided into seven main clades. In the *Hymenochaetaceae* clade, *S. lonicericola*, *S. weigelae*, and *S. alpinus* exhibited a close relationship and clustered into a common subclade. This study illustrates the complexity of mitochondrial genomes among five *Sanghuangporus* species, providing information useful for the development of potential molecular markers for phylogenetic analyses as well as for further elucidating the evolutionary history, functional implications, and underlying mechanisms of these medicinal mushrooms.

Supplementary Information

The online version contains supplementary material available at https://doi.org/10.1186/s12864-026-12832-6.

Supplementary Material 1. Table S1 The analyzed internal transcribed spacer (ITS) sequences of the *Sanghuangporus* species used in this study. Table S2 Basidiomycota mitochondrial genome information. Table S3 Quality control metrics for three newly assembled *Sanghuangporus* mitochondrial genomes. Table S4 Simple sequence repeats (SSRs) in the five *Sanghuangporus* mitochondrial genomes. Table S5 Interspersed repeats in the five *Sanghuangporus* mitochondrial genomes. Table S6 Tandem repeats in the five *Sanghuangporus* mitochondrial genomes. Table S7 Potential RNA-editing sites in the protein-coding genes (PCGs) of the five *Sanghuangporus* mitochondrial genomes. Table S8 Amino acid changes in the potential RNA-editing sites of the protein-coding genes (PCGs) in the five *Sanghuangporus* mitochondrial genomes. Fig. S1 Phylogenetic tree inferred from *Sanghuangporus* internal transcribed spacer (ITS) sequences. Fig. S2 Quantitative assembly validation metrics for the three *Sanghuangporus* species. Fig. S3 Syntenic blocks identified by Mauve, showing the correspondence between alignment blocks and genes. Fig. S4 Comparative visualization of mitogenomic similarity alignments in the five *Sanghuangporus* species. Fig. S5 Distribution of repeat elements in the mitochondrial genome of *Sanghuangporus weigelae*. The outermost circle represents simple sequence repeats (SSRs), followed by tandem repeats, while the lines (pink/blue) in the innermost circle denote interspersed forward (F) and palindromic (P) repeats. Fig. S6 Gene arrangements involving tRNA genes labeled with the abbreviations of their corresponding amino acids. Fig. S7 Inferred secondary structures of 26 tRNAs of *Sanghuangporus weigelae* and unique tRNAs in the other four *Sanghuangporus* mitochondrial genomes. The tRNAs are labeled with the abbreviations of their corresponding amino acids. Gray-colored dots (●) indicate Watson-Crick base pairing, and black-colored dots (●) indicate *–U base pairing. Fig. S8 Unique tRNA structures in *Sanghuangporus sanghuang* and *S. vaninii*.

Acknowledgements

We thank the Editors and the anonymous reviewers for their insightful comments and suggestions on the manuscript.

Authors' contributions

C.J: Data curation, Formal analysis, Investigation, Methodology, Software, Visualization, Writing-original draft, Writing-review & editing. Y.Y.J: Formal analysis, Methodology, Software, Visualization, Writing-original draft. L.X.T: Formal analysis, Methodology, Software, Visualization, Writing-original draft. J.X.M: Formal analysis, Methodology, Software, Visualization, Writing-original draft. X.L: Visualization, Writing-original draft. J.S: Conceptualization, Data curation, Formal analysis, Funding acquisition, Investigation, Project administration, Resources, Supervision, Validation, Writing-original draft, Writing-review & editing. B.K.C: Conceptualization, Data curation, Funding acquisition, Investigation, Project administration, Resources, Supervision, Validation, Writing-review & editing.

Funding

This study was supported by the National Natural Science Foundation of China (32270016, 32470002, 32070016, and 32325001) and the Beijing Nova Program (20230484322).

Data availability
The mitochondrial genome data are available through the NCBI under project number PV558911–PV558913. Data generated or analyzed during this study are included in this published article and its supplementary information files. The mitochondrial genome datasets used during the current study will be made available from the corresponding author on reasonable request.

Declarations

Ethics approval and consent to participate
All materials used in this study comply with international and national legal standards. The collected species material does not pose a threat to other species, and the collection of the species is recognized by the relevant authorities.

Consent for publication
Not applicable.

Competing interests
The authors declare no competing interests.

Received: 7 October 2025 / Accepted: 1 April 2026
Published online: 22 April 2026

References

1. Dai YC. Hymenochaetaceae (Basidiomycota) in China. Fungal Divers. 2010;45:131–343. https://doi.org/10.1007/s13225-010-0066-9.
2. Zhou LW, Vlasák J, Decock C, Assefa A, Stenlid J, Abate D, Wu SH, Dai YC. Global diversity and taxonomy of the *Inonotus linteus* complex (Hymenochaetales, Basidiomycota): *Sanghuangporus* gen. nov., *Tropicoporus excentrodendri* and *T. guanacastensis* gen. et spp. nov., and 17 new combinations. Fungal Divers. 2016;77:335 – 47. https://doi.org/10.1007/s13225-015-0335-8
3. Xu TM, Wu DM, Gao N, Liu S, Sun YF, Cui BK. Species diversity, taxonomic classification and ecological habits of polypore fungi in China. Mycology. 2025;16:419–544. https://doi.org/10.1080/21501203.2024.2384567.
4. De Silva DD, Rapior S, Fons F, Bahkali AH, Hyde KD. Medicinal mushrooms in supportive cancer therapies: an approach to anti-cancer effects and putative mechanisms of action. Fungal Divers. 2012;55:1–35. https://doi.org/10.1007/s13225-012-0151-3.
5. De Silva DD, Rapior S, Hyde KD, Bahkali AH. Medicinal mushrooms in prevention and control of diabetes mellitus. Fungal Divers. 2012;56:1–29. https://doi.org/10.1007/s13225-012-0187-4.
6. De Silva DD, Rapior S, Sudarman E, Stadler M, Xu JC, Alias SA, Hyde KD. Bioactive metabolites from macrofungi: ethnopharmacology, biological activities and chemistry. Fungal Divers. 2013;62:1–40. https://doi.org/10.1007/s13225-013-0265-2.
7. Wang H, Ma JX, Zhou M, Si J, Cui BK. Current advances and potential trends of the polysaccharides derived from medicinal mushrooms sanghuang. Front Microbiol. 2022;13:965934. https://doi.org/10.3389/fmicb.2022.965934.
8. Wang H, Ma JX, Wu DM, Gao N, Si J, Cui BK. Identifying bioactive ingredients and antioxidant activities of wild *Sanghuangporus* species of medicinal fungi. J Fungi. 2023;9:242. https://doi.org/10.3390/jof9020242.
9. Guo L, Liu YG, Fu YW, Wang YY, Wang HJ, Zhu SM, He QZ, Zhang DX, Zhu SS, Wang SX, Tong T, Dong XJ, Wang XL, Liu YN, Liu GQ. Multiomics reveals the molecular mechanism of unsaturated fatty acid-induced terpenoid biosynthesis in *Sanghuangporus lonicericola*. npj Sci Food. 2025;9:44. https://doi.org/10.1038/s41538-025-00407-w.
10. Pfanner N, Warscheid B, Wiedemann N. Mitochondrial proteins: from biogenesis to functional networks. Nat Rev Mol Cell Biol. 2019;20:267–84. https://doi.org/10.1038/s41580-018-0092-0.
11. Burger G, Gray MW, Lang BF. Mitochondrial genomes: anything goes. Trends Genet. 2003;19:709–16. https://doi.org/10.1016/j.tig.2003.10.012.
12. Najer T, Doña J, Bucek A, Sweet AD, Sychra O, Johnson KP. Mitochondrial genome fragmentation is correlated with increased rates of molecular evolution. PLoS Genet. 2024;20:e1011266.https://doi.org/10.1371/journal.pgen.1011266.
13. Tang JT, Zhang LL, Su JH, Ye QW, Li YK, Liu DH, Cui HF, Zhang YF, Ye ZH. Insights into fungal mitochondrial genomes and inheritance based on current findings from yeast-like gungi. J Fungi. 2024;10:441. https://doi.org/10.3390/jof10070441.
14. Skippington E, Barkman TJ, Rice DW, Palmer JD. Miniaturized mitogenome of the parasitic plant *Viscum scurruloideum* is extremely divergent and dynamic and has lost all *nad* genes. PNAS. 2015;112. https://doi.org/10.1073/pnas.1504491112. E3515 – 24.
15. Zhang X, Li PH, Wang J, Fu DX, Zhao BP, Dong WX, Liu YX. Comparative genomic and phylogenetic analyses of mitochondrial genomes of Hawthorn (*Crataegus* spp.) in Northeast China. Int J Biol Macromol. 2024;272:132795. https://doi.org/10.1016/j.ijbiomac.2024.132795.
16. Wang L, Liu X, Xu YJ, Zhang ZW, Wei YS, Hu Y, et al. Assembly and comparative analysis of the first complete mitochondrial genome of a traditional Chinese medicine *Angelica biserrata* (Shan et Yuan) Yuan et Shan. Int J Biol Macromol. 2024;257:128571. https://doi.org/10.1016/j.ijbiomac.2023.128571.
17. Wang Z, Wang RN, Sang YT, Wang T, Su YJ, Liao WB. Comparative analysis of mitochondrial genomes of invasive weed *Mikania micrantha* and its indigenous congener *Mikania cordata*. Int J Biol Macromol. 2024;281:136357. https://doi.org/10.1016/j.ijbiomac.2024.136357.
18. Paijmans JLA, Gilbert MTP, Hofreiter M. Mitogenomic analyses from ancient DNA. Mol Phylogenet Evol. 2013;69:404–16. https://doi.org/10.1016/j.ympev.2012.06.002.
19. Ghiselli F, Gomes-dos-Santos A, Adema CM, Lopes-Lima M, Sharbrough J, Boore JL. Molluscan mitochondrial genomes break the rules. Philos Trans R Soc Lond B Biol Sci. 2021;376:20200159. https://doi.org/10.1098/rstb.2020.0159.
20. Kristjansson D, Bohlin J, Nguyen TT, Jugessur A, Schurr TG. Evolution and dispersal of mitochondrial DNA haplogroup U5 in Northern Europe: insights from an unsupervised learning approach to phylogeography. BMC Genom. 2022;23:354. https://doi.org/10.1186/s12864-022-08572-y.
21. Feofilova EP. The kingdom fungi: Heterogeneity of physiological and biochemical properties and relationships with plants, animals, and prokaryotes (review). Appl Biochem Microbiol. 2001;37:124–37. https://doi.org/10.1023/A:1002863311534.
22. Li Q, Xiang DB, Wan Y, Wu Q, Wu XY, Ma CR, et al. The complete mitochondrial genomes of five important medicinal *Ganoderma* species: Features, evolution, and phylogeny. Int J Biol Macromol. 2019;139:397–408. https://doi.org/10.1016/j.ijbiomac.2019.08.003.
23. Agnestisia R, Ono A, Nakamura L, Chino R, Nodera K, Aiso-Sanada H et al. The complete mitochondrial genome sequence of the medicinal fungus *Inonotus obliquus* (*Hymenochaetaceae*, Basidiomycota). Mitochondrial DNA B Resour. 2019;4:3504 – 6. https://doi.org/10.1080/23802359.2019.1675548
24. He QX, Jiang YX, Li YL, Guan TZ, Jing XL, Meng C. Complete mitochondrial genome sequencing and phylogenetic analysis of *Phellinus igniarius*. Sci Rep. 2024;14:31109. https://doi.org/10.1038/s41598-024-82372-0.
25. Han JG, Oh J, Jo JW, Kim CS, Kwag YN, Han SK, et al. The complete mitochondrial genome of *Sanghuangporus sanghuang* (Hymenochaetaceae, Basidiomycota). Mitochondrial DNA B Resour. 2018;3:456–7. https://doi.org/10.1080/23802359.2018.1462116.
26. Song TT, Xu F, Shen YY, Fan LJ, Cai WM. The complete mitochondrial genome of *Sanghuangporus vaninii* Zhehuang-1 (Hymenochaetales, Basidiomycota). Mitochondrial DNA B Resour. 2021;6:1096–7. https://doi.org/10.1080/23802359.2020.1832592.
27. Kulik T, Van Diepeningen AD, Hausner G, Editorial. The significance of mitogenomics in mycology. Front Microbiol. 2021;11:628579. https://doi.org/10.3389/fmicb.2020.628579.
28. Kouvelis VN, Hausner G. Editorial: mitochondrial genomes and mitochondrion related gene insights to fungal evolution. 2022;13:897981. https://doi.org/10.3389/fmicb.2022.897981
29. Kolesnikova AI, Putintseva YA, Simonov EP, Biriukov VV, Oreshkova NV, Pavlov IN, et al. Mobile genetic elements explain size variation in the mitochondrial genomes of four closely-related *Armillaria* species. BMC Genom. 2019;20:351. https://doi.org/10.1186/s12864-019-5732-z.
30. Jin C, Ma JX, Wang H, Tang LX, Ye YF, Li X, Si J. First genome assembly and annotation of *Sanghuangporus weigelae* uncovers its medicinal functions, metabolic pathways, and evolution. Front Cell Infect Microbiol. 2024;13:1325418. https://doi.org/10.3389/fcimb.2023.1325418.
31. Chen SF. Ultrafast one-pass FASTQ data preprocessing, quality control, and deduplication using fastp. iMeta. 2023;2:e107. https://doi.org/10.1002/imt2.107.
32. Jin JJ, Yu WB, Yang JB, Song Y, dePamphilis CW, Yi TS, Li DZ. GetOrganelle: a fast and versatile toolkit for accurate de novo assembly of organelle

genomes. Genome Biol. 2020;21:241. https://doi.org/10.1186/s13059-020-02154-5.
33. Kolmogorov M, Bickhart DM, Behsaz B, Gurevich A, Rayko M, Shin SB, et al. metaFlye: scalable long-read metagenome assembly using repeat graphs. Nat Methods. 2020;17:1103–10. https://doi.org/10.1038/s41592-020-00971-x.
34. Hu J, Wang Z, Sun ZY, Hu BX, Ayoola AO, Liang F, et al. NextDenovo: an efficient error correction and accurate assembly tool for noisy long reads. Genome Biol. 2024;25:107. https://doi.org/10.1186/s13059-024-03252-4.
35. Lang BF, Beck N, Prince S, Sarrasin M, Rioux P, Burger G. Mitochondrial genome annotation with MFannot: a critical analysis of gene identification and gene model prediction. Front Plant Sci. 2023;14:1222186. https://doi.org/10.3389/fpls.2023.1222186.
36. Donath A, Jühling F, Al-Arab M, Bernhart SH, Reinhardt F, Stadler PF, et al. Improved annotation of protein-coding genes boundaries in metazoan mitochondrial genomes. Nucleic Acids Res. 2019;47:10543–52. https://doi.org/10.1093/nar/gkz833.
37. Tillich M, Lehwark P, Pellizzer T, Ulbricht-Jones ES, Fischer A, Bock R, Greiner S. GeSeq-versatile and accurate annotation of organelle genomes. Nucleic Acids Res. 2017;45. https://doi.org/10.1093/nar/gkx391. W6 – 11.
38. Chan PP, Lin BY, Mak AJ, Lowe TM. tRNAscan-SE 2.0: improved detection and functional classification of transfer RNA genes. Nucleic Acids Res. 2021;49:9077–96. https://doi.org/10.1093/nar/gkab688.
39. Edera AA, Small I, Milone DH, Sanchez-Puerta MV. Deepred-Mt: Deep representation learning for predicting C-to-U RNA editing in plant mitochondria. Comput Biol Med. 2021;136:104682. https://doi.org/10.1016/j.compbiomed.2021.104682.
40. Alikhan NF, Petty NK, Ben Zakour NL, Beatson SA. BLAST Ring Image Generator (BRIG): simple prokaryote genome comparisons. BMC Genom. 2011;12:402. https://doi.org/10.1186/1471-2164-12-402.
41. Darling ACE, Mau B, Blattner FR, Perna NT. Mauve: multiple alignment of conserved genomic sequence with rearrangements. Genome Res. 2004;14:1394–403. https://doi.org/10.1101/gr.2289704.
42. Frazer KA, Pachter L, Poliakov A, Rubin EM, Dubchak I. VISTA: computational tools for comparative genomics. Nucleic Acids Res. 2004;32. https://doi.org/10.1093/nar/gkh458. W273 – 9.
43. Beier S, Thiel T, Münch T, Scholz U, Mascher M. MISA-web: a web server for microsatellite prediction. Bioinformatics. 2017;33:2583–5. https://doi.org/10.1093/bioinformatics/btx198.
44. Benson G. Tandem repeats finder: a program to analyze DNA sequences. Nucleic Acids Res. 1999;27:573–80. https://doi.org/10.1093/nar/27.2.573.
45. Kurtz S, Choudhuri JV, Ohlebusch E, Schleiermacher C, Stoye J, Giegerich R. REPuter: the manifold applications of repeat analysis on a genomic scale. Nucleic Acids Res. 2001;29:4633–42. https://doi.org/10.1093/nar/29.22.4633.
46. Krzywinski M, Schein J, Birol I, Connors J, Gascoyne R, Horsman D, et al. Circos: An information aesthetic for comparative genomics. Genome Res. 2009;19:1639–45. https://doi.org/10.1101/gr.092759.109.
47. Tamura K, Stecher G, Kumar S. MEGA11: molecular evolutionary genetics analysis version 11. Mol Biol Evol. 2021;38:3022–7. https://doi.org/10.1093/molbev/msab120.
48. Zhang Z. KaKs_Calculator 3.0: calculating selective pressure on coding and non-coding sequences. Genom Proteom Bioinf. 2022;20. https://doi.org/10.1016/j.gpb.2021.12.002. :536 – 40.
49. Zhang D, Gao FL, Jakovlić I, Zou H, Zhang J, Li WX, Wang GT. PhyloSuite: An integrated and scalable desktop platform for streamlined molecular sequence data management and evolutionary phylogenetics studies. Mol Ecol Resour. 2020;20:348–55. https://doi.org/10.1111/1755-0998.13096.
50. Rozas J, Ferrer-Mata A, Sánchez-DelBarrio JC, Guirao-Rico S, Librado P, Ramos-Onsins SE, et al. DnaSP 6: DNA sequence polymorphism analysis of large data sets. Mol Biol Evol. 2017;34:3299–302. https://doi.org/10.1093/molbev/msx248.
51. Sharp PM, Li WH. Codon usage in regulatory genes in *Escherichia coli* does not reflect selection for 'rare' codons. Nucleic Acids Res. 1986;14:7737–49. https://doi.org/10.1093/nar/14.19.7737.
52. Kalyaanamoorthy S, Minh BQ, Wong TKF, von Haeseler A, Jermiin LS. ModelFinder: fast model selection for accurate phylogenetic estimates. Nat Methods. 2017;14:587–9. https://doi.org/10.1038/nmeth.4285.
53. Lanfear R, Frandsen PB, Wright AM, Senfeld T, Calcott B. PartitionFinder 2: new methods for selecting partitioned models of evolution for molecular and morphological phylogenetic analyses. Mol Biol Evol. 2017;34:772–3. https://doi.org/10.1093/molbev/msw260.
54. Xia XH. DNA replication and strand asymmetry in prokaryotic and mitochondrial genomes. Curr Genom. 2012;13:16–27. https://doi.org/10.2174/138920212799034776.
55. Fonseca PLC, De-Paula RB, Araujo DS, Tome LMR, Mendes-Pereira T, Rodrigues WFC, Del-Bem LE, Aguiar ERGR, Goes-Neto A. Global characterization of fungal mitogenomes: new insights on genomic diversity and dynamism of coding genes and accessory elements. Front Microbiol. 2021;12:787283. https://doi.org/10.3389/fmicb.2021.787283.
56. Hugaboom M, Hatmaker EA, LaBella AL, Rokas A. Evolution and codon usage bias of mitochondrial and nuclear genomes in *Aspergillus* section *Flavi*. G3-Genes. Genom Genet. 2022;13:jkac285. https://doi.org/10.1093/g3journal/jkac285.
57. Sandor S, Zhang YJ, Xu JP. Fungal mitochondrial genomes and genetic polymorphisms. Appl Microbiol Biotechnol. 2018;102:9433–48. https://doi.org/10.1007/s00253-018-9350-5.
58. Kashi Y, King DG. Simple sequence repeats as advantageous mutators in evolution. Trends Genet. 2006;22:253–9. https://doi.org/10.1016/j.tig.2006.03.005.
59. Ahmad A, Wang JD, Pan YB, Sharif R, Gao SJ. Development and use of simple sequence repeats (SSRs) markers for sugarcane breeding and genetic studies. Agronomy. 2018;8:260. https://doi.org/10.3390/agronomy8110260.
60. Aguileta G, de Vienne DM, Ross ON, Hood ME, Giraud T, Petit E, Gabaldón T. High variability of mitochondrial gene order among fungi. Genome Biol Evol. 2014;6:451–65. https://doi.org/10.1093/gbe/evu028.
61. Férandon C, Moukha S, Callac P, Benedetto JP, Castroviejo M, Barroso G. The *Agaricus bisporus cox*1 gene: the longest mitochondrial gene and the largest reservoir of mitochondrial group I introns. PLoS ONE. 2010;5:e14048. https://doi.org/10.1371/journal.pone.0014048.
62. Meiklejohn C, Montooth K, Rand D. Positive and negative selection on the mitochondrial genome. Trends Genet. 2007;23. https://doi.org/10.1016/j.tig.2007.03.008. :259 – 63.
63. Liu Y, Yang Q, Zhao FZ. Synonymous but not silent: the codon usage code for gene expression and protein folding. Annu Rev Biochem. 2021;90:375–401. https://doi.org/10.1146/annurev-biochem-071320-112701.
64. Moss MJ, Chamness LM, Clark PL. The effects of codon usage on protein structure and folding. Annu Rev Biophys. 2024;53:87–108. https://doi.org/10.1146/annurev-biophys-030722-020555.
65. Liu Y. A code within the genetic code: codon usage regulates co-translational protein folding. Cell Commun Signal. 2020;18:145. https://doi.org/10.1186/s12964-020-00642-6.
66. Fuglsang A. Impact of bias discrepancy and amino acid usage on estimates of the effective number of codons used in a gene, and a test for selection on codon usage. Gene. 2008;410:82–8. https://doi.org/10.1016/j.gene.2007.12.001.
67. Jühling F, Pütz J, Bernt M, Donath A, Middendorf M, Florentz C, Stadler PF. Improved systematic tRNA gene annotation allows new insights into the evolution of mitochondrial tRNA structures and into the mechanisms of mitochondrial genome rearrangements. Nucleic Acids Res. 2012;40:2833–45. https://doi.org/10.1093/nar/gkr1131.
68. Salinas-Giegé T, Giegé R, Giegé P. tRNA biology in mitochondria. Int J Mol Sci. 2025;16:4518–59. https://doi.org/10.3390/ijms27010367.
69. Brennicke A, Marchfelder A, Binder S. RNA editing. FEMS Microbiol Rev. 1999;23:297–316. https://doi.org/10.1111/j.1574-6976.1999.tb00401.x.
70. Lo Giudice C, Hernández I, Ceci LR, Pesole G, Picardi E. RNA editing in plants: a comprehensive survey of bioinformatics tools and databases. Plant Physiol. 2013;161:1240–8. https://doi.org/10.1104/pp.112.213116.
71. Kotera E, Tasaka M, Shikanai T. A pentatricopeptide repeat protein is essential for RNA editing in chloroplasts. Nature. 2005;433:326–30. https://doi.org/10.1038/nature03229.
72. Williams TA, Cox CJ, Foster PG, Szöllősi GJ, Embley TM. Phylogenomics provides robust support for a two-domains tree of life. Nat Ecol Evol. 2020;4:138–47. https://doi.org/10.1038/s41559-019-1040-x.

Publisher's note